

Generalised ultrafast dispersion scans of continuum generation induced by sub-50fs chirped pulses in highly nonlinear tapered planar waveguides

Matthew Praeger, William S. Brocklesby, Ana M. De Paula, Jeremy Frey, and Jeremy J. Baumberg,

School of Physics, University of Southampton, Southampton SO17 1BJ, United Kingdom,
Caterina M. Netti, Majd E. Zoorob, Nicolas M. B. Perney, Martin D. B. Charlton, Stephen W. Roberts, James S. Wilkinson, Gregory J. Parker, and John R. Lincoln,

Mesophotonics Ltd, 2 Venture Road, Chilworth Science Park, Southampton, SO16 7NP, United Kingdom

ABSTRACT

Ultra-high bandwidth continua generated by ultrashort fs pulses have been attracting enormous interest for applications such as general spectroscopy, Optical Coherence Tomography and metrology. Dispersion engineering is one of the key aspects of optimised continuum generation in optical waveguides. However in addition, the dispersion of the pump pulse can be continuously adapted to control bandwidth and spectral characteristics of the generated continua. In this work we report on a systematic investigation of how 2nd and 3rd order dispersion affects the continuum generated in strongly non linear planar waveguides. A ~30 fs Ti:Sapphire tuned to 800 nm was used as a pump source delivering ~3 nJ pulses. The chirp of the pulses was controlled completely-arbitrarily by an acousto-optic programmable dispersive filter (Dazzler). The power launched into the structures was kept constant to compare the generated continua as the pulse dispersion is varied. High refractive index tantalum pentoxide (Ta_2O_5) waveguides grown by standard silicon processing techniques were used. The devices investigated were specially designed tapered ridges with ~5 mm² input modal volume and zero group velocity dispersion at ~1-3.7 mm. Self-phase modulation, which is responsible for the spectral broadening of the continua, is tracked by finely tuning the both 2nd and 3rd order dispersions. The nonlinear propagation is dramatically influenced by the simultaneous presence of these dispersive effects resulting in a change of bandwidth and spectral shape. Pulse widths of up to $\Delta\lambda > 100$ nm for launched powers as low as 300 pJ. Spectral peak intensity can also be systematically modulated by simply scanning the 2nd and 3rd order dispersion around their relative zeros. Specific combinations of high order dispersion contribution are currently targeted as a route to control and optimise the continua bandwidths and to control dispersion lengths in specifically engineered waveguides.

Keywords: Continuum, Dispersion, Dazzler, Self-Phase, Tantalum-Pentoxide,

1. INTRODUCTION

This paper presents experimental results on continuum generation in high-refractive-index tantalum pentoxide (Ta_2O_5) waveguides. The experiment has two main aims, to measure the spectral broadening of the continuum as a function of input laser power and to measure the effects of input pulse dispersion on the continuum generation process. Power is controlled by a variable reflecting neutral density filter (see section 5). Control of the input pulse dispersion is through the use of an acousto-optic programmable dispersive filter (AOPDF) (see section 3). During the course of this work planar, rib and ridge waveguides have all been studied with waveguide lengths of between 3 and 10 mm and widths in the range of 1000–5000 nm. The results presented here also show the effect of tapering the centre section of the waveguide.

Further author information:

M. Praeger: E-mail: mattp@soton.ac.uk,

C. Netti: E-mail: caterina.netti@mesophotonics.com

2. EXPERIMENTAL CONFIGURATION

The laser used in this experiment was a Kerr lens modelocked Ti:Sapphire capable of generating approximately 30 fs pulses. By varying input pump power and adjusting the prism translation inside the laser it is possible to slightly alter the power and the spectrum of the output beam. However typical values are approximately 40 nm bandwidth at just over 300 mW average power. The energy per pulse is approximately 3nJ and therefore peak powers of the order of 1.0×10^5 W can be achieved.

Figure 1 shows a schematic representation of the typical experimental setup.

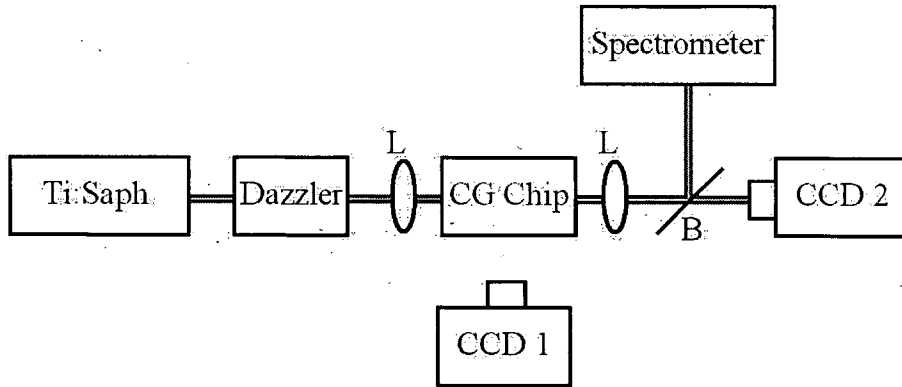


Figure 1. Schematic diagram of the apparatus used in this experiment.

Upon exiting the laser the beam passes through the AOPDF (the Dazzler) which can be used to alter arbitrarily the dispersion of the pulses. A brief explanation of how the Dazzler does this is provided in section 3.

The coupling system consists of 2 high precision X Y Z translation stages used to align the input and output couplers to the beam. The CG chip was mounted on a 4 axis stage allowing full control of chip alignment. A CCD camera with a zoom lens was mounted above the 4 axis stage to give a plan view of the CG chip (see figure 4). Once the CG chip is aligned the output light (the continuum) can be collected and imaged with the output coupler. A beamsplitter was used to send part of the beam to the spectrometer whilst a second CCD camera is used to image the output facet of the chip (see figure 2).

Output mode profiles.

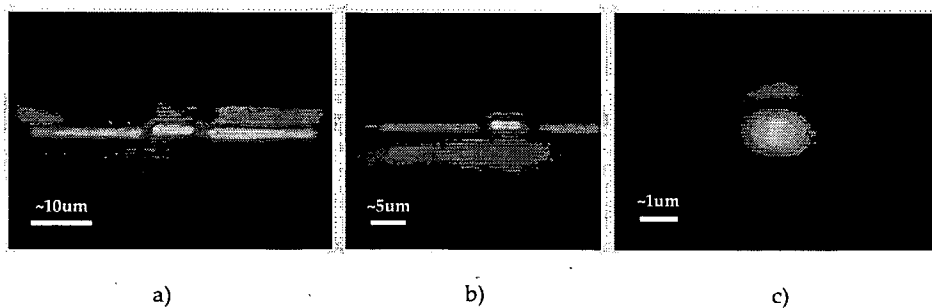


Figure 2. a) A poorly coupled wider rib 3 lobes can be observed. b) $3\mu\text{m}$ – $6\mu\text{m}$ wide ribs tend to exhibit 2 lobes when poorly aligned. c) Ribs narrower than $\sim 2\mu\text{m}$ are single mode. The lack of additional scattered light indicates that this rib is well coupled. Note: The scale change between the images.

A moulded glass aspheric lens (effective focal length: 3.1 mm, NA: 0.68) is used as the input coupler. A telescope was used to control the beam collimation and size at the focusing optic. The second CCD camera was used to optimise alignment for propagation in a particular mode. Some example images are shown in figure 2a,b and c. All alignment was done at low power, as it is possible to damage the chip if too much power is coupled into the silicon substrate.

3. DAZZLER

The Dazzler (Fastlite) is an example of an acousto-optic programmable dispersive filter as described in reference.¹ The Dazzler crystal enables us to arbitrarily alter the second and higher order dispersion of the laser beam.

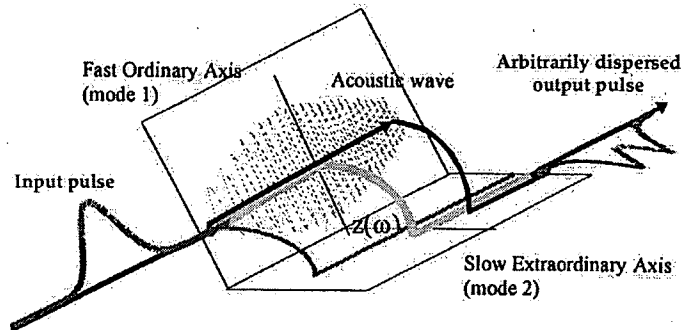


Figure 3. This diagram (taken from reference²) shows the operation of the Dazzler crystal.

The general premise of the Dazzler's operation is as follows: A short laser pulse is launched into the Dazzler crystal in mode 1 and a radio frequency acoustic wave propagates through the crystal along the same axis. The acoustic wave modulates the crystal lattice spacing to create an acoustic grating with spatial frequency proportional to the frequency of the acoustic wave. This acoustic grating can diffract light out of mode 1 and into mode 2 where it sees a higher refractive index and therefore propagates more slowly. The grating only diffracts one particular optical wavelength efficiently, given by the acoustic spatial frequency. It is therefore possible, by controlling the shape and timing of the acoustic wave, to diffract different wavelengths into mode 2 at different depths through the crystal. The total time for each wavelength to propagate through the crystal can therefore be controlled (see figure 3). The amplitude of the acoustic wave also allows control of how much light is diffracted into mode 2.

Using this effect the phase and amplitude of different spectral components of the pulse can be arbitrarily controlled. The output beams from modes 1 and 2 are spatially and angularly separated making it easy to select only the mode 2 beam to be sent to the experiment.

The Dazzler was calibrated using a frequency resolved optical grating (FROG). The Dazzler value that compensated best for the dispersion in our laser system and produced the shortest pulse was taken to be the zero point of second order dispersion ($0 fs^2$). All figures quoted here for second order dispersion are relative to this measured zero point.

4. TANTALA PENTOXIDE WAVEGUIDES

The waveguides discussed here are produced using standard silicon manufacturing technologies with RF sputtering, e-beam lithography and plasma etching. Each continuum generation chip is a small section (typically $3\text{ mm} \times 10\text{ mm} \times 1\text{ mm}$) of silicon wafer with the $3\text{ mm} \times 1\text{ mm}$ faces polished to form the input and output facets.

In this experiment the waveguiding medium deposited on top of the silicon wafer is high refractive index ($n \sim 2.1$ at 800 nm) tantala pentoxide (Ta_2O_5). A protective cover layer of silicon dioxide is also added.

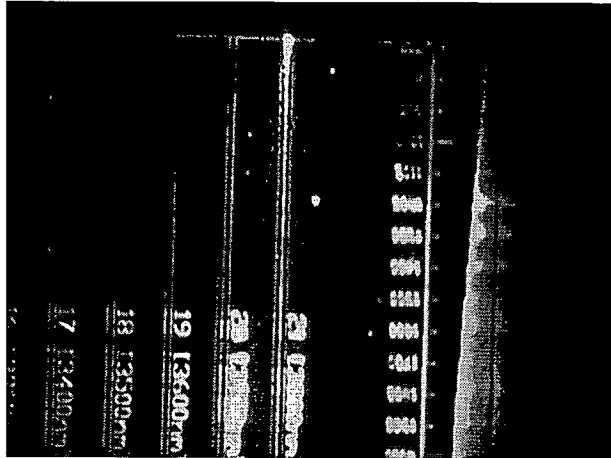


Figure 4. Plan view CCD image showing a coupled rib.

In some of the CG chips the waveguides taper or expand to a centre section that is either narrower or wider than the input facet. The high production quality of these chips is evident in figure 4.

5. POWER DEPENDENCE

In this part of the experiment the power dependence of the CG process was measured. A variable ND wheel was used as this made it possible to adjust the laser power without significantly altering CG chip coupling.

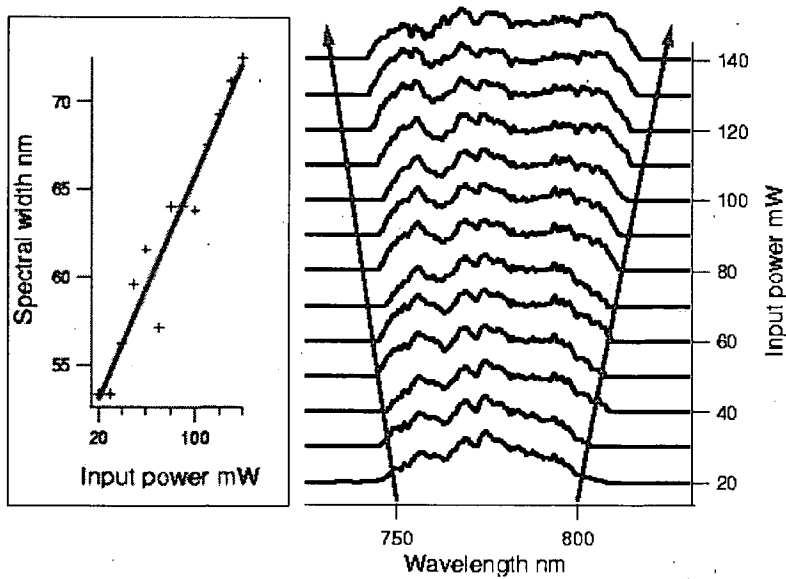


Figure 5. Output spectra from a 1 μm wide rib over a range of input laser powers. The inset shows spectral width as a function of input power.

Figure 5 shows data that was collected using a $1\ \mu\text{m}$ wide rib waveguide. For these experiments, the Dazzler was set to give a second order dispersion of $+2000\ \text{fs}^2$ and third order dispersion of $0\ \text{fs}^3$. Since continuum generation is the result of a nonlinear effect (self-phase modulation) it is expected that the higher the power density inside the chip can be made the greater the broadening that will be observed. This trend is clearly observed in figure 5.

Additional confinement of the guided light can be used to increase power densities which further enhances the nonlinear effect, hence the progression from planar waveguides to rib type structures. Tapered ribs are now in use that combine relatively large facets (for efficient coupling) with narrow centre sections that strongly confine the mode causing increased power density.

6. SECOND ORDER DISPERSION

Increasing the second order dispersion of the laser pulses has an obvious effect on the optical power density that is created in the CG chip, significantly reducing the peak power density as the pulse length is increased.

The dispersion that occurs during propagation inside the CG chip must also be taken into consideration. For example in a tapered rib it may be advantageous to launch a slightly negatively-chirped pulse into the rib. As the pulse propagates through the rib it will be compressed spectrally by the normal dispersion of the waveguide medium whilst at the same time being spatially compressed by the tapering of the waveguide. Scanning the pulse dispersion allows this to be tested.

The Dazzler (see section 3) was used to scan the second order dispersion of the input laser whilst spectra were taken. The results for two different ribs are shown in figures 6 and 7.

These figures show spectra along the horizontal axis (lighter tone indicates more intensity at that wavelength). The vertical axis shows the second order dispersion variation using the Dazzler. The spectra have been normalised to the same peak intensity by taking the log of the spectral intensity then subtracting the peak value.

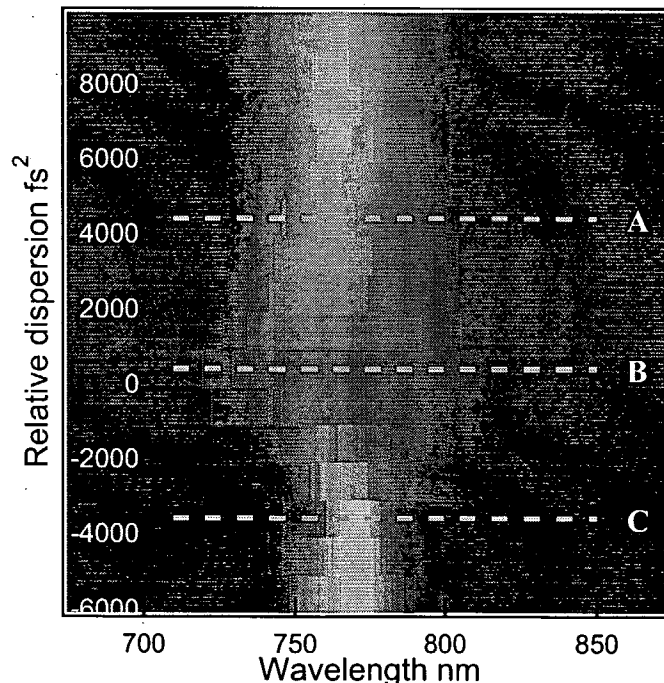


Figure 6. Output spectra from a $1.8\ \mu\text{m}$ wide CG rib as a function of 2^{nd} order dispersion. Third order = $-2.0 \times 10^4\ \text{fs}^3$.

Figure 6 shows the response of a straight $1.8 \mu\text{m}$ wide CG rib. Second order has been scanned whilst the third order dispersion has been fixed at $-2.0 \times 10^4 \text{ fs}^3$. Broadening is clearly increased for second order dispersion values near to the relative 0 fs^2 . The broadening is approximately symmetric, similar to that seen as the power is varied, and probably represents the variation on peak power as the pulse is lengthened by the chirp.

Figure 7 shows the response of a tapered rib. The facets of the rib are $2.8 \mu\text{m}$ wide but then taper over $\sim 1 \text{ mm}$ to a straight centre section of $1.8 \mu\text{m}$ width. This rib behaves similarly to the untapered one in that the best broadening again occurs near to 0 fs^2 . However, the broadening is now no longer symmetric.

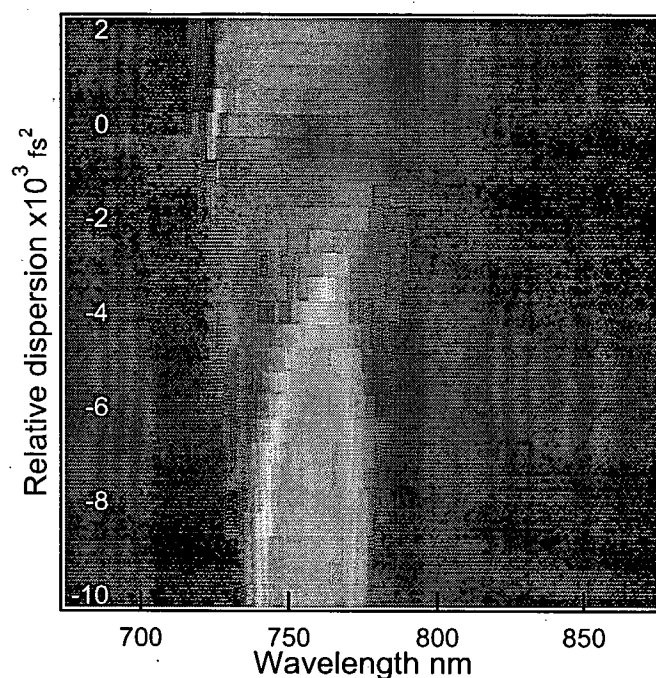


Figure 7. Output spectra from a tapered rib (with $1.8 \mu\text{m}$ wide centre section) as a function of 2^{nd} order dispersion. Third order = 0 fs^3 .

The broadening occurs near to 0 fs^2 (our measured value for the relative zero of dispersion) since this value compensates for the dispersion in the system, and produces the shortest pulse (and therefore highest peak power) within the CG chip.

An interesting feature of figure 7 is that for the tapered waveguide, the spectrum does not evolve in the same way as would be expected for a simple change in peak power. The variation of second order dispersion shows asymmetric wavelength dependence, with the peak shifting to longer wavelength just below the zero of second order dispersion, and moving to shorter wavelength just above the zero. It has been proposed³ that this feature may provide a means to measure the nonlinear refraction and absorption of bulk material or waveguide samples.

7. THIRD ORDER DISPERSION

The same $1 \mu\text{m}$ untapered rib as was used for figure 6 was used here. For three different values of second order dispersion (indicated by the lines A, B and C on figure 6) the third order dispersion was scanned and output spectra recorded.

The effect of the third order dispersion is significantly different from and more subtle than that of the second order. Figures 8 and 9 show the effect of scanning third order dispersion for positive ($+4400 \text{ fs}^2$) and negative

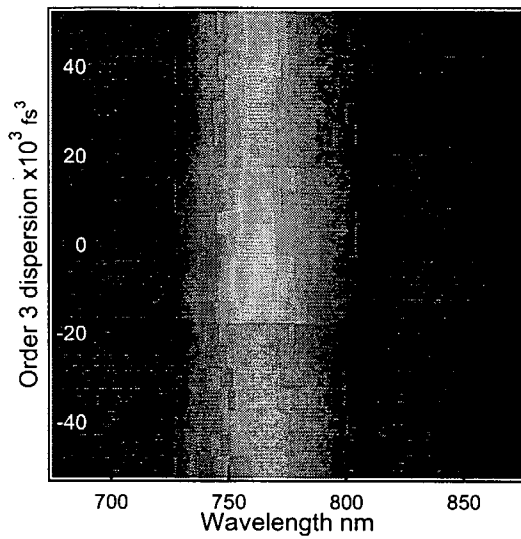


Figure 8. (Line A on figure 6) Output spectra from a $1\mu\text{m}$ wide CG rib vs 3^{rd} order dispersion. Second order = $+4400\text{ fs}^2$ (relative).

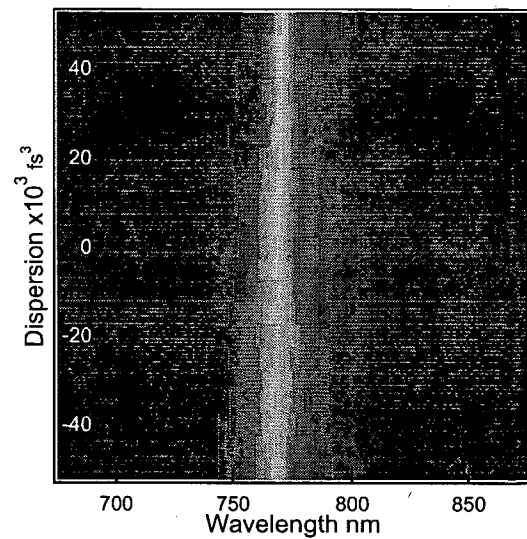


Figure 9. (Line C on figure 6) Output spectra from a $1\mu\text{m}$ wide CG rib vs 3^{rd} order dispersion. Second order = -3600 fs^2 (relative).

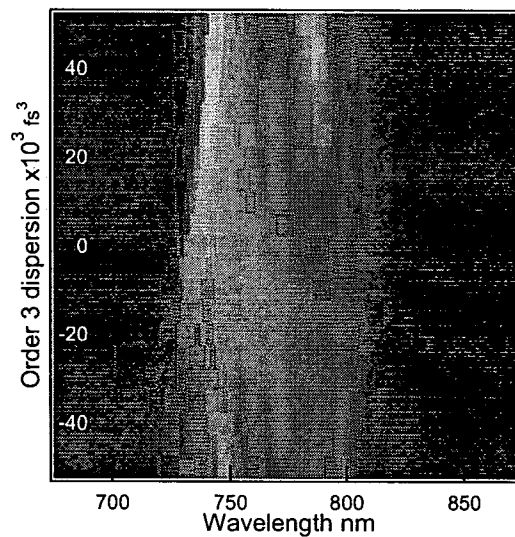


Figure 10. (Line B on figure 6) Output spectra from a $1\mu\text{m}$ wide CG rib vs 3^{rd} order dispersion. Second order = $+400\text{ fs}^2$ (relative).

(-3600 fs^2) second order dispersion respectively. In figure 10 the second order dispersion is set very near to the relative zero value ($+400\text{ fs}^2$).

It seems that for a positive second order dispersion, large negative third order dispersion results in a spectral broadening to longer wavelengths. Conversely for a negative second order, negative third order dispersion broadens spectrum towards shorter wavelengths.

Near to the relative zero of second order dispersion in figure 10 the third order dispersion has a more noticeable effect on the broadening of the spectrum. It seems that the third order dispersion must be carefully controlled in order to obtain the optimum broadening.

8. SUMMARY

In summary, this experiment has investigated the performance of CG chips and in particular the study of their dispersion dependant properties using the Dazzler crystal. Results demonstrating the power dependence of the continuum generation process have been included, as has a comparison of the effects of second order dispersion in two types of waveguide (straight and tapered with tapered waveguides exhibiting an enhanced response). Finally, results demonstrating the effects of third order dispersion at three different values of second order dispersion (in the same waveguide) have been presented. It has been shown that both second and third order dispersion have an appreciable effect upon the spectral broadening that can be achieved through self-phase modulation in waveguides. In addition, the Dazzler has been demonstrated to be a highly effective method of scanning and controlling pulse dispersion in order to sample and then optimise the performance of dispersion sensitive optical elements. In order to fully optimise the performance of continuum generation devices it is necessary to consider these dispersion effects; theoretical understanding of these effects can be put to use in the design of future devices. The addition of photonic crystals to the waveguides will further allow control of both the generation and dispersion properties of the system, allowing comprehensive control of the spectral output.

REFERENCES

1. D. Kaplan and P. Tournois, "Theory and performance of the acousto optic programmable dispersive filter used for femtosecond laser pulse shaping," *Journal De Physique Iv* **12**(PR5), pp. 69-75, 2002. 580XF J PHYS IV.
2. F. Verluise, V. Laude, Z. Cheng, C. Spielmann, and P. Tournois, "Amplitude and phase control of ultrashort pulses by use of an acousto-optic programmable dispersive filter: pulse compression and shaping," *Optics Letters* **25**(8), pp. 575-577, 2000. 304UD OPTICS LETTERS.
3. F. Louradour, E. Lopez-Lago, V. Couderc, V. Messager, and A. Barthelemy, "Dispersive-scan measurement of the fast component of the third- order nonlinearity of bulk materials and waveguides," *Optics Letters* **24**(19), pp. 1361-1363, 1999.